Supplementary Materials

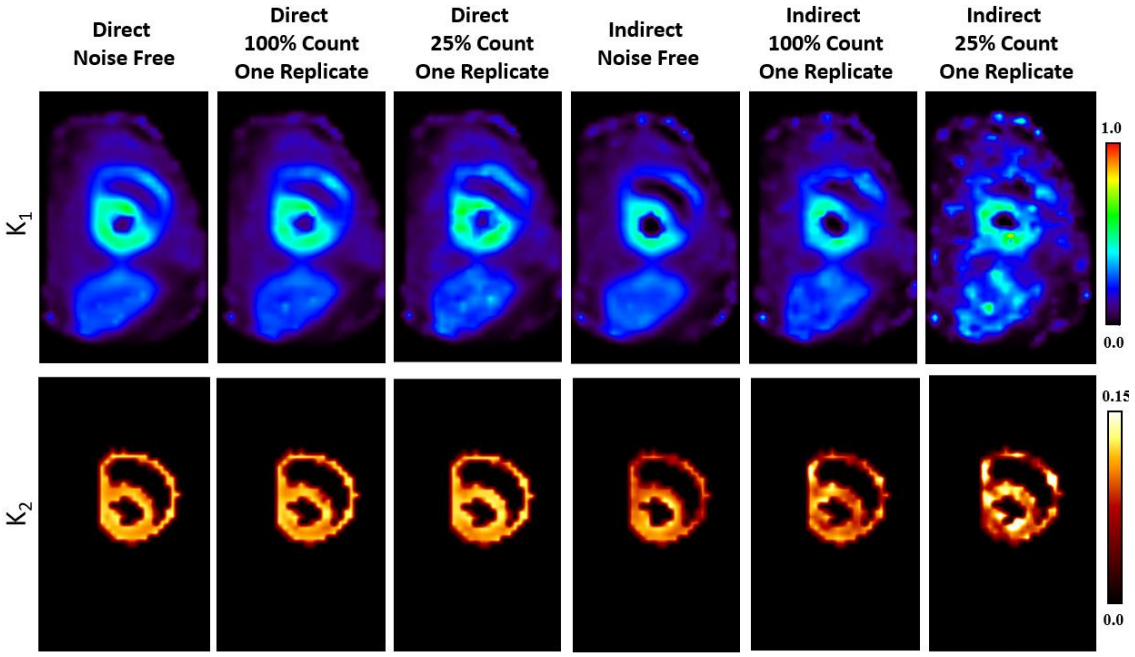

Fig. S1. K_1 and k_2 parametric images generated from simulated canine data by direct and indirect methods for the three groups: noise free, 100%-count and 25%-count noisy simulations. For each of the two noisy groups, only one replicate sample image is given. The images were compared at iteration 80. The k_2 images were masked to the myocardium, since k_2 provides less relevant information outside of myocardium.

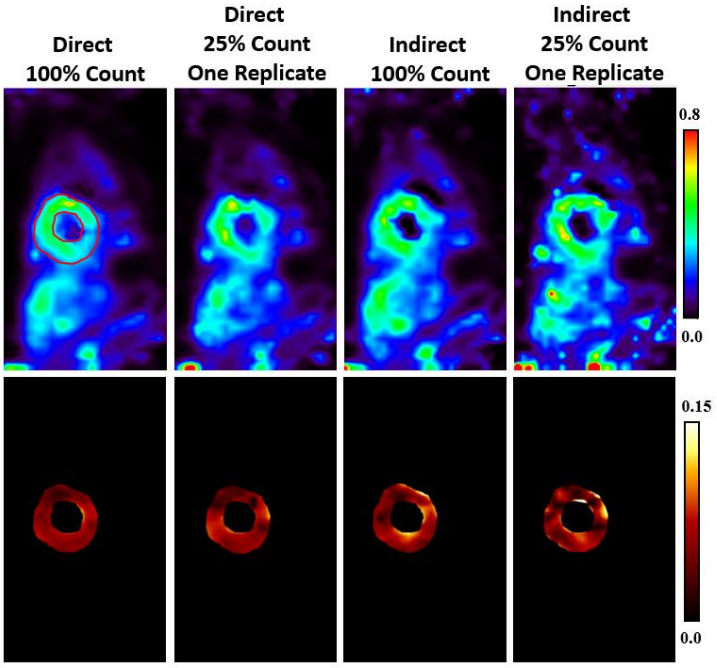

Fig. S2. K_1 and k_2 parametric images generated by direct and indirect methods for the 100%-count and 25%-count *in vivo* canine data. For each 25% low-count group, only one replicate sample image is given. The images were compared at iteration 80. The k_2 images were masked to the LV myocardium segmented from the 100%-count direct K_1 images (shown by the red circles), since k_2 provides less relevant information outside of myocardium.

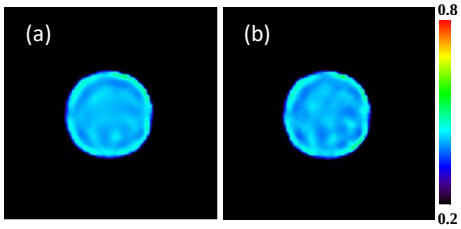

Fig. S3. K_1 parametric images of the cylinder simulation generated by direct (a) and indirect (b) approaches at iteration 100. The 4D dynamic phantom was created using a 3D uniform cylinder phantom with diameter 120 mm and height 120 mm. The 1-tissue (1T) model was used to describe the tracer kinetics, with K_1, k_2 and V_L set to 0.4 $\text{mL} \cdot \text{min}^{-1}$, 0.1 min^{-1} and 0, respectively. The total counts in this 20-min simulation were about 38.6 million. The same initializations were used as in Section III.A for both direct and indirect methods. Since Point Spread Function (PSF) was incorporated into the system matrix, Gibbs artifacts can be observed on both images.

Table SI. Comparison between direct and indirect results for the noise-free cylinder simulation. The measurement ROI (cylinder shape with diameter 40mm and height 8mm) was placed in the center of the simulated cylinder to minimize the effect from Gibbs artifacts and partial volume on our measurement.

@ Iter 100	K_1	$K_{1,\text{uncorr}}$	k_2	V_L
Direct	0.4097	0.4015	0.1013	0.0202
Indirect	0.4087	0.4032	0.1009	0.0136
Ground Truth	0.4	0.4	0.1	0

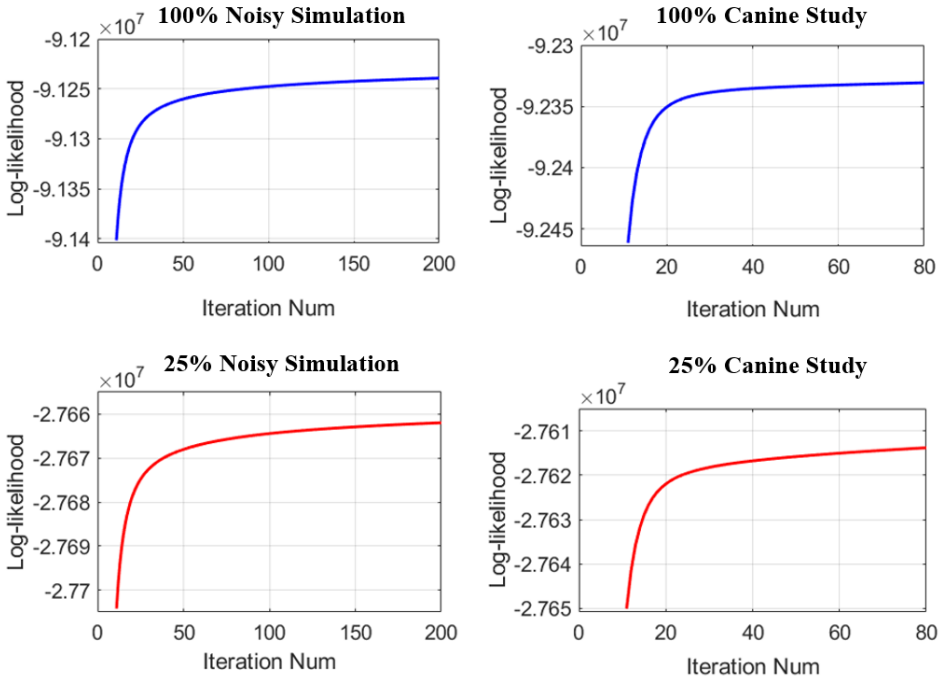

Fig. S4. Example plots of the log-likelihood functions for the direct method. Only one replicate was shown for the noisy simulations and the 25% low-count canine study. The ground-truth input function and 100% input function were used in the 25% noisy simulation and 25% canine study, respectively. The log-likelihood function is defined in Eq.(S1). We omitted the first 10 iterations to focus on the later-iteration dynamic range.

The log-likelihood function, i.e., the very function we are optimizing, is defined as:

$$\log g = \sum_{it} \left\{ -\Delta t \sum_{j} c_{ij} A_i L_t \left[K_{1,\mathrm{uncorr},j} \sum_{\tau=0}^{t} C_{\mathrm{L}}(\tau)\, e^{-k_{2,j}(t-\tau)} + V_{\mathrm{L},j} C_{\mathrm{L}}(t) \right] \right.$$
$$\left. + \mathrm{y}_{it} \log \left(\Delta t \sum_{j} c_{ij} A_i L_t \left[K_{1,\mathrm{uncorr},j} \sum_{\tau=0}^{t} C_{\mathrm{L}}(\tau)\, e^{-k_{2,j}(t-\tau)} + V_{\mathrm{L},j} C_{\mathrm{L}}(t) \right] \right) \right\} \qquad \text{(S1)}$$

Example plots of the log-likelihood functions for the direct method are shown in Fig. S4.